Journal of Material Cycles and Waste Management (2024) 26:2152–2158
https://doi.org/10.1007/s10163-024-01954-2

ORIGINAL ARTICLE

# Speciation of antimony and vanadium in municipal solid waste incineration ashes analyzed by XANES spectroscopy

**Christian Vogel[1] · Philipp Scholz[1] · Ute Kalbe[1] · Wolfgang Caliebe[2] · Akhil Tayal[2] · Sami Juhani Vasala[3] · Franz-Georg Simon[1]**

Received: 7 November 2023 / Accepted: 1 April 2024 / Published online: 2 May 2024


## Abstract

The use of ashes from municipal solid waste incineration as secondary building materials is an important pillar for the circular economy in Germany. However, leaching of potential toxic elements from these materials must be at environmentally acceptable levels. Normally, a three-month ageing period immobilizes most hazardous heavy metals, but antimony (Sb) and vanadium (V) showed previously unusual leaching. In order to clarify the mechanisms, we analyzed the Sb and V species in various bottom and fly ashes from municipal waste incineration by XANES spectroscopy. Antimony oxidizes from Sb(+ III) species used as flame retardants in plastics to Sb(+ V) compounds during waste incineration. However, owing to the similarity of different Sb(+ V) compound in the Sb K- and L-edge XANES spectra, it was not possible to accurately identify an exact Sb(+ V) species. Moreover, V is mainly present as oxidation state + V compound in the analyzed ashes. However, the coarse and magnetic fraction of the bottom ashes contain larger amounts of V(+ III) and V(+ IV) compounds which might enter the waste incineration from vanadium carbide containing steel tools. Thus, Sb and V could be critical potential toxic elements in secondary building materials and long-term monitoring of the release should be taken into account in the future.

**Keywords** Heavy metals · Potential toxic elements (PTEs) · X-ray absorption near-edge structure (XANES) spectroscopy

## Introduction

Since 1896 solid waste incineration is applied to the reduction of the volume and germ destruction of municipal solid waste in Germany [1]. Nowadays around 100 solid waste incineration plants are in operation in Germany. These plants generated approx. six million tons of municipal solid waste incineration—bottom ash (BA) in Germany annually [2]. In addition, an estimated annual accumulation of approx. 640,000 tons of fly ash (FA) occurs [3]. After iron and non-ferrous oxide metals separation, the BA contain still some non-ferrous metals and the mineral fraction (90%), in which the metals with a high affinity for oxygen (silicon, calcium, aluminum, magnesium, etc.) are bound in oxidic form [4]. Because their composition is similar to mineral raw materials the BAs can be used as secondary building material [5]. Until the BAs can be used e.g. as subbase material in road construction [6], they have to pass a three-month ageing period (Best Available Techniques (BAT) Reference Document for Waste Incineration, EUR 29971 EN). During this period, the pH value of the BAs gradually decreases, and pollutants are immobilized by processes like carbonation. In particular, leaching of potential toxic elements (PTEs) is reduced to environmentally acceptable levels.

To analyze the long-term leaching behavior of PTEs in BAs a lysimeter experiment was performed with treated BA for almost 6 years [7]. As expected, the leaching of most heavy metals as well as chloride and sulfate decreased as a function of the liquid-to-solid ratio (L/S in L/kg) in the lysimeter experiment. In contrast to that, the leaching of antimony (Sb) and vanadium (V) increased over time. The explanation for this behavior was that Sb and V leaching is low as long as the concentration of calcium ions (Ca) is high

✉ Christian Vogel
christian.vogel@bam.de

[1] Division 4.3 Contaminant Transfer and Environmental Technologies, Bundesanstalt für Materialforschung und -prüfung (BAM), Unter den Eichen 87, 12205 Berlin, Germany

[2] Deutsches Elektronen-Synchrotron DESY, Notkestrasse 85, 22607 Hamburg, Germany

[3] ESRF - The European Synchrotron, 71 Avenue des Martyrs, 38000 Grenoble, France

enough to precipitate most Sb and V as sparingly soluble Ca-antimonates and -vanadates. Decreasing Ca ion concentrations as a result of BA ageing ($CaCO_3$ formation which is almost insoluble from CaO and $Ca(OH)_2$ in the presence of $CO_2$ from the atmosphere or natural rain) leads to dissolution of these antimonates and vanadates [7, 8].

Antimony is a critical element, which under natural conditions occurs in two oxidation states—Sb(+ III) and Sb(+ V). In accordance to experiments and clinical trials on antimony, the virulence of Sb(+ III) is ten times that of Sb(+ V) [9]. However, released Sb(+ V) from secondary building materials can sorb onto inorganic oxides and organic matter in soils which may affect environmental health by ecotoxic effects and bioaccessibility [9–11].Vanadium has acquired significant attention as a PTE due to its extensive use in various industrial applications. However, it is important to note that compounds containing V in the oxidation state + V have been found to exhibit ecotoxic effects when introduced into the environment [12–14]. In addition, for both Sb and V information on the environmental impact are still rare [15].

Therefore, the aim of this study was to analyze various BAs and one FA by X-ray absorption near-edge structure (XANES) spectroscopy to determine the chemical state and bonding of Sb and V to estimate their potential hazard. Owing to the little spectral features in the Sb K-edge [16–18] and V K-edge [13, 19, 20] spectrum of conventional XANES spectroscopy, we also applied high energy resolution fluorescence detected (HERFD-)XANES spectroscopy [21]. Moreover, we additionally applied the Sb $L_1$-edge [22, 23] and Sb $L_3$-edge XANES spectroscopy [24–26], respectively.

## Materials and methods

### Sampling

Four BAs and one FA from various municipal solid waste incineration (MSWI) plants in Germany were analyzed in this study. BA1 and BA3 were sampled at municipal waste incineration (MSWI) plants in northern Germany with grate technology and wet ash extraction systems. BA2 was sampled at a MSWI plant in southern Germany where the water supply of the extraction system was stopped and dry bottom ash was sampled. BA4 was sampled at an industrial incineration plant treating substitute fuel. FA1 stemmed from a waste incinerator where a multicyclone is placed between the boiler and spray dryer so that no flue gas cleaning products are contained in this fly ash. Furthermore, from BA3, the coarse fraction (> 16 mm) was additionally used. Moreover, from the investigated BAs the magnetic fraction (BA-M) was separated and also analyzed. In addition, we investigated a BA used in a long-term lysimeter leaching test (BA-L) for almost 6 years [7].

The mass fractions (in mg per kg dry weight) of Sb and V and other elements in the samples were analyzed by ICP-OES (Thermo iCAP 7000, Dreieich, Germany) after microwave-assisted aqua regia digestion ($HNO_3$/HCl; mikroPrepA, MLS GmbH, Leutkirch, Germany). All digestions and ICP-OES measurements were carried out in triplicates.

### Antimony (Sb) X-ray absorption near-edge structure (XANES) spectroscopy

Antimony K-edge XANES spectroscopy measurements were carried out at P64 beamline [27] at the electron storage ring PETRA III (DESY, Hamburg, Germany). The incident beam was monochromatized with a Si < 311 > double crystal monochromator. The scans were performed at room temperature. The Sb K-edge XANES spectra were collected in the range of 30240–31490 eV with a passivated implanted planar silicon (PIPS) detector in fluorescence mode.

The Sb $L_1$- and $L_3$-edge XANES spectroscopy measurements were carried out at ID26 beamline in the TEXS chamber [28] at the electron storage ring ESRF (Grenoble, France). The incident beam was monochromatized with a Si < 111 > double crystal monochromator. An emission spectrometer with five crystal analyzers (5 × Si < 311 > , $R$ = 1 m for Sb Lα1 detection; 5 × Si < 220 > , R = 1 m for Sb Lα3) in the ultra-high vacuum TEXS chamber was selected to have to obtain a strong characteristic fluorescence line around the maximum intensity (bandwidth around 1.7 and 2.0 eV, respectively). This detection method results in higher resolution spectral features (HERFD-XANES spectroscopy) and optimal suppression of background. The scans were performed at 50 K, to reduce radiation damage in the sample. The XANES scan range was 4393–4723 eV at the Sb $L_1$-edge and 4110–4210 eV at the Sb $L_3$-edge, respectively. The data from ESRF are stored in the ESRF data portal [29].

### Vanadium (V) K-edge XANES spectroscopy

The V K-edge XANES spectroscopy measurements were also carried out at ID26 beamline at the electron storage ring ESRF (Grenoble, France) using a Si < 111 > double crystal monochromator. An emission spectrometer with five crystal analyzers (5 × Ge < 331 > , $R$ = 1 m for V Kα detection) within a helium bag, to decrease the scattering from air, was used for the most optimal bandwidth (bandwidth around 1.2 eV). The scans were also acquired at 50 K, to reduce radiation damage in the sample. The XANES scan range was 5450–5550 eV.

### XANES data handling

All spectra were background subtracted and normalized to an edge jump of Δμd = 1 using the Athena software from the Demeter 0.9.26 package (Ravel and Newville 2005). In addition, the Sb and V K-edge XANES spectra were analyzed with linear combination (LC) fitting [30]. The spectral fitting range was set from – 50 to + 150 eV of the Sb K-edge and -10 to + 50 eV of the V K-edge, respectively. The maximum number of compounds in the final LC fit was limited to three and the sum of the compounds was forced to add up to 100%. From all possible LC fits the combination with the lowest R value was chosen.

The following Sb reference compounds ($Sb_2O_3$, $Sb_2S_3$, $SbCl_3$), $Sb_2(SO_4)_3$, $Sb_2O_5$ (all Sigma-Aldrich), $NaSbF_6$ (> 95%, ThermoFisher), and $Ca(Sb(OH)_6)_2$. which was precipitated from $KSb(OH)_6$ (for analysis, BerndKraft) [17], were applied for the LC fits. Furthermore, all V K-edge XANES spectra ($V_2O_3$ (≥ 99%, Carl Roth), $VCl_3$ (97%, Aldrich), VC (99%, Alfa Aesar), $V_2O_5$ (99.99%, Alfa Aesar), $CaV_2O_6$ was precipitated from $NH_4VO_3$ (> 99.8%, Carl Roth) [31] except for $NH_4VO_3$ were used for LC fitting.

## Results and discussion

### Antimony and vanadium contents of investigated BAs and FA

The analyzed mass fractions of Sb and V in various MSWI ashes are shown in Table 1 (the whole analysis is displayed in Table S1). The Sb values of the BAs are in the range 35.0–86.3 mg/kg. The analyzed FA exhibited a significantly higher concentration of Sb (539.9 mg/kg) as compared to the investigated BAs. This finding is consistent with previous studies indicating that fly ashes generally contain higher levels of pollutants compared to bottom ashes [32]. In contrast, the vanadium concentration in the FA is not increase in comparison to the BAs. The V mass fractions are between 21.3 and 51.1 mg/kg, but the > 16 mm fraction of BA3 has an enriched V content of 101.5 mg/kg.

**Table 1** Sb and V mass fractions in (mg/kg) of various MSWI bottom ashes (BAs) and a fly ash (FA)

| | Sb (mg/kg) MV ± SD | V (mg/kg) MV ± SD |
|---|---|---|
| FA1 | 539.9 ± 1.5 | 44.1 ± 0.0 |
| BA1 | 38.3 ± 0.2 | 23.4 ± 2.5 |
| BA2 | 50.7 ± 2.7 | 42.0 ± 2.6 |
| BA3 | 86.3 ± 1.4 | 21.3 ± 1.0 |
| BA 3> 16 mm | 35.0 ± 1.0 | 101.5 ± 5.5 |
| BA4 | 37.8 ± 1.1 | 38.8 ± 0.0 |
| BA-L | 85.5 ± 2.6 | 51.1 ± 0.4 |
| BA-M | 52.8 ± 3.7 | 56.7 ± 1.3 |

*BA-L* bottom ash after lysimeter experiment, *BA-M* magnetic fraction of bottom ashes, *MV* mean value, *SD* standard deviation

### Antimony XANES spectroscopy of MSWI ashes

Figure 1 shows the Sb K-edge XANES spectra of various pure Sb compounds (top) and the investigated BAs and FA (bottom). All Sb(+ III) and Sb(+ V) compounds, respectively, look very similar in the Sb K-edge XANES spectrum. But the Sb(+ III) compounds show an absorption edge at 30492 eV, while Sb(+ V) compounds exhibit the edge at 30497 eV. In addition, the Sb(+ V) compounds display an additional shoulder at 30514 eV.

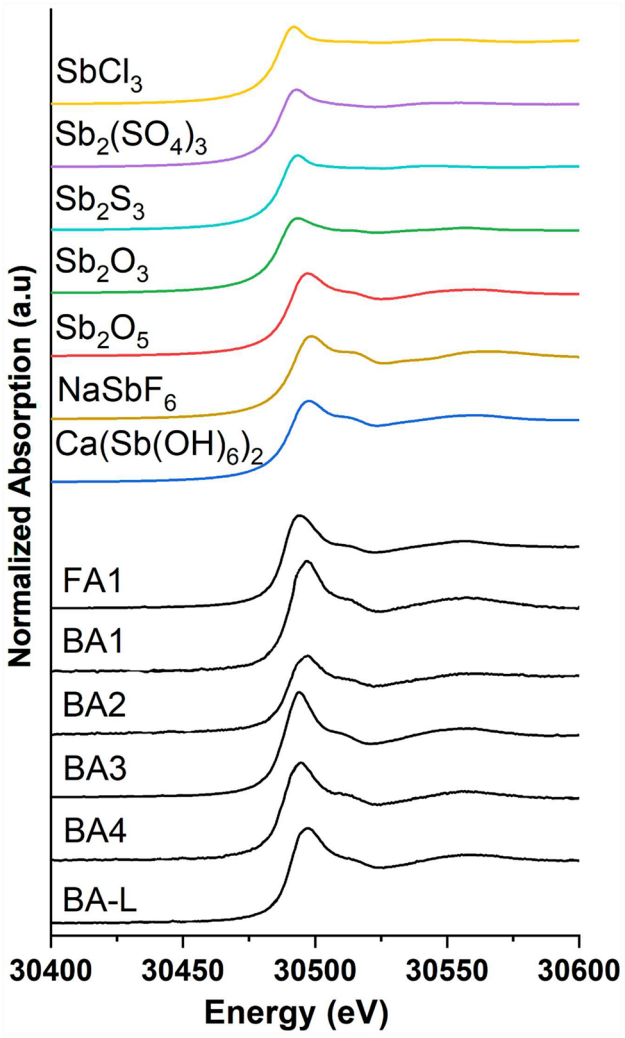


**Fig. 1** Antimony K-edge XANES spectra of various Sb references (top) as compared to various bottom ashes (BAs) and a fly ash (FA) (bottom)

The analyzed BAs and FA show an absorption edge shifted to higher energies with higher oxidation state and a whiteline (most intense absorption) at the Sb(+V) region and the additional feature at 30514 eV (see Fig. 1 bottom). This indicates that the ash residues contain significantly more Sb(+V) compounds compared to Sb(+III). Although the spectra of the Sb(+III) and Sb(+V) compounds are very similar we applied linear combination (LC) fitting for further analysis to the sample spectra (see best fit results in Table S2). The LC fits confirm that Sb(+V) compounds are the major Sb compound of all investigates ashes.

For further analysis we also applied Sb $L_1$-edge (Fig. 2) and Sb $L_3$-edge (Fig. S1) XANES spectroscopy to the samples. Because of the low Sb content of the ashes, only a spectrum for FA1 could be collected at the Sb $L_1$-edge, which again confirms the Sb(+V) dominance in that sample. The spectra of FA1 and BA1 at the Sb $L_3$-edge (Fig. S1) are noisier, however, Sb(+V) related features are detectable there as well.

Sources of Sb in municipal waste incineration are mainly flame retardants from plastics [33]. Plastics often contain between 200 and 300 mg/kg of Sb [34]. Therefore, we also analyzed plastic material containing $Sb_2O_3$/$SnO_2$ as flame retardant [35] using Sb $L_1$-edge XANES spectroscopy (see Fig. 2). The XANES spectrum clearly identifies a Sb(III) compound. This was also confirmed by the Sb $L_3$-edge XANES spectroscopy (see Fig. S1). Thus, during municipal solid waste incineration, Sb(+III) containing plastics will be oxidized to Sb(+V) compounds.

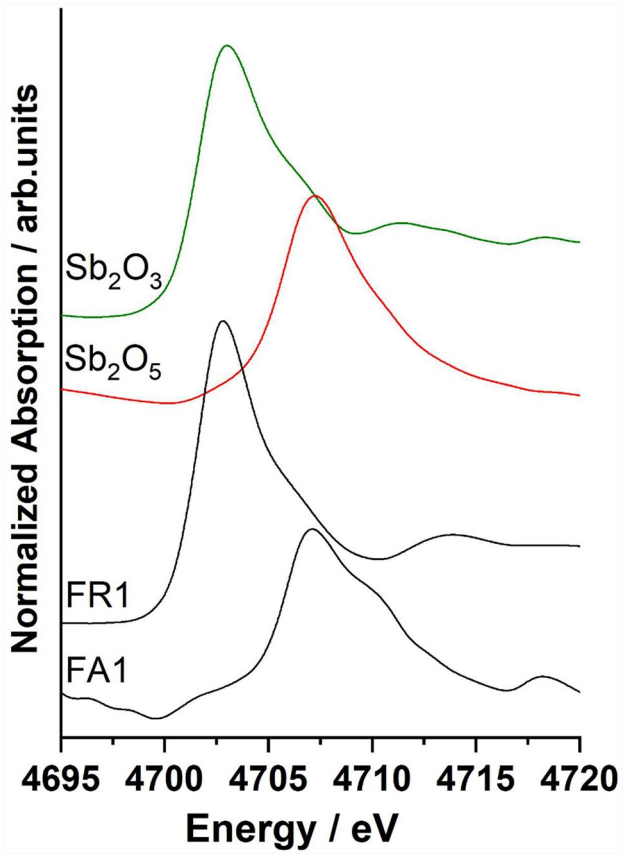


**Fig.2** Antimony $L_1$-edge HERFD-XANES spectra of Sb containing plastic as flame retardant (FR1) and fly ash 1 (FA1)

Previously, calcium antimonate $Ca(Sb(OH)_6)_2$ was assumed to be the major Sb compound in BAs [7, 36]. However, this could not finally be proved, because the Sb XANES spectra of $Sb_2O_5$ and $Ca(Sb(OH)_6)_2$ at all accessed edges are too similar for a clear differentiation, since in both compounds Sb(V) compounds antimony is directly surrounded by oxygen atoms.

Moreover, the wet-mechanically treated BA in a lysimeter (BA-L) for almost 6 years [7] was also analyzed and showed also only Sb(+V) compounds (LC fit in Table S1). Thus, the Sb in BA-L remained in oxidation state +V and no reduction from Sb(+V) to Sb(+III) was detectable over the long period of 6 years, which confirms the unusual leaching behavior of Sb during the long-term leaching process.

## Vanadium XANES spectroscopy of MSWI ashes

In Fig. 3, V K-edge XANES spectra of the V reference compounds (top) and the analyzed BAs and FA (bottom) are presented. Because of the applied V K-edge HERFD-XANES spectroscopy, in contrast to conventional XANES spectroscopy, a pre-peak at 5470 eV [37] for the V(+III) compounds is shown as well. However, the rising absorption edge for the V(III) compounds occurs at a lower energy than for the V(+IV) and V(+V) compounds, respectively. Especially, $VCl_3$ shows a much more prominent whiteline (most intense absorption) than the other compounds (see Fig. 3).

The V K-edge XANES spectra of the investigated BAs 1–4 and FA look very similar. The LC fits of the spectra (see Table S2) indicate a majority of the V(+V) compound $CaV_2O_6$, supplemented by a minor part of the V(+III) compound $VCl_3$ for all samples. In contrast, the > 16 mm fraction of BA3, which is enriched in V and other metals (see Table 1), contains a larger V(+III) fraction (see Table S3). This is in accordance with the V K-edge XANES spectrum, which shows a whiteline which best fits with $VCl_3$ or VC. A similar feature was obtained in the spectrum of the magnetic fraction of the BAs (BA-M). The LC fit again also indicates some V(+IV) for BA-M in addition to V(+V) and V(+III) compounds (see Table S2). However, due to the noise level of the spectrum, the *R*-value is low. The V(+IV) species VC is used in industry for steel hardening for the increased demand for high grade steel worldwide [14, 38]. Moreover, because of its great hardness and temperature resistance [39] VC is commercially used for tool bits and cutting tools. After their end-of-lifetime these tools may enter the municipal solid waste incineration and remains in the magnetic

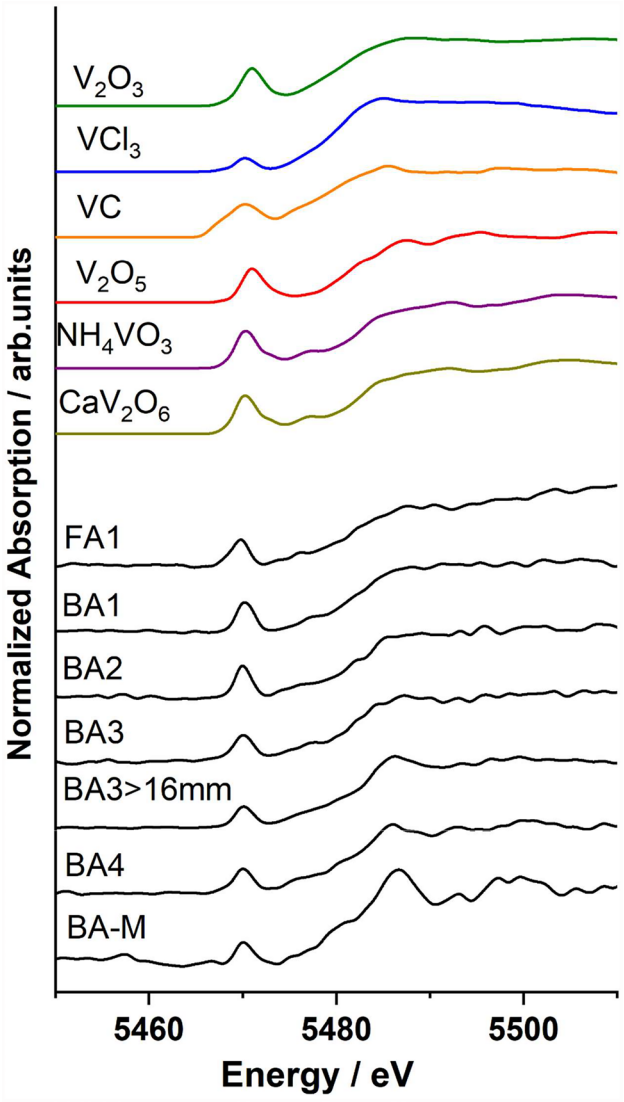


**Fig.3** Vanadium K-edge HERFD-XANES spectra of vanadium references (top) as compared to various bottom ashes and a fly ash (bottom)

fraction of the BAs. Therefore, V containing tools may be an important source for V in waste incineration BAs and possibly also into the environment.

## Conclusion

Our XANES investigation showed that various BAs and an FA contain mainly Sb and V in the oxidation state + V. For Sb the exact Sb(+ V) species could not be identified even though we applied it on three different Sb XANES edges, because all investigated Sb(+ V) compounds used for LC fits contain Sb directly surrounded by oxygen which result into very similar spectra. From the experimental results it is obvious that Sb used as component within flame retardant systems for plastic materials will be oxidized to Sb(+ V) during MSWI. Due to the presence of large quantities of Ca in BAs and FAs it is not unlikely that Ca-antimonate was formed, which is sparingly soluble as far as enough Ca ions are available.

For V some fractions of the BAs showed larger amounts of V(+ III) and V(+ IV) compounds which may enter MSWI plants as steel hardener in tools bits and cutting tools. In the case of V(+V) a similar mechanism regarding precipitation and dissolution as for Sb takes place [7, 8].

The input of Sb and V to the process of MSWI cannot be suppressed completely. Therefore, BAs and FAs will also contain Sb and V in the future. For FA this is a lesser problem because at least in Germany FAs are backfilled underground with no contact to rain or surface water. In contrast to that, BAs are utilized throughout Europe to a larger extent as secondary building material [40]. This could require some long-term monitoring for the protection of the environment. However, even in a 6 years lysimeter experiment [7] the limit values as set in the German Secondary Building Material Ordinance [41] were not exceeded.

**Supplementary Information** The online version contains supplementary material available at https://doi.org/10.1007/s10163-024-01954-2.

**Acknowledgements** We thank Bernhard Schartel (BAM) for provision of the flame retardant containing plastic.

**Funding** Open Access funding enabled and organized by Projekt DEAL. The authors thank the German Environment Agency (UBA, FKZ 3720333050) for funding. We acknowledge DESY (Hamburg, Germany), a member of the Helmholtz Association HGF, for the provision of experimental facilities. Parts of this research were carried out at PETRA III and we would like to thank the local staff for assistance in using P64 beamline. Beamtime was allocated for proposal I-20220046. Furthermore, we acknowledge the European Synchrotron Radiation Facility (ESRF) for provision of synchrotron radiation facilities under proposal number EV-511 and we would like to thank for the support in using the beamline.

**Data availability** The datasets used and/or analyzed during the current study are available from the corresponding author on reasonable request.

## References


1. Holm O, Simon F-G (2017) Innovative treatment trains of bottom ash (BA) from municipal solid waste incineration (MSWI) in Germany. Waste Manage 59:229–236. https://doi.org/10.1016/j.wasman.2016.09.004
2. ITAD Jahresbericht 2021 (Annual report 2021) (2021) ITAD—Interessengemeinschaft der Thermischen Abfallbehandlungsanlagen in Deutschland e.V: Düsseldorf
3. Statistisches Bundesamt (2020) Erhebung der Abfallentsorgung, Tabelle 31111-0004
4. Bayuseno AP, Schmahl WW (2010) Understanding the chemical and mineralogical properties of the inorganic portion of MSWI bottom ash. Waste Manag 30(8):1509–1520. https://doi.org/10.1016/j.wasman.2010.03.010
5. Singh P, Boora A, Kumar Gupta A (2023) A review on utilizing municipal solid waste incineration (MSWIA) in construction activates. IOP Conf Ser Earth Environ Sci. 1110(1):012042. https://doi.org/10.1088/1755-1315/1110/1/012042
6. Di Gianfilippo M, Hyks J, Verginelli I, Costa G, Hjelmar O, Lombardi F (2018) Leaching behaviour of incineration bottom ash in a reuse scenario: 12years-field data vs. lab test results. Waste Manag 73:367–380. https://doi.org/10.1016/j.wasman.2017.08.013
7. Simon F-G, Vogel C, Kalbe U (2021) Antimony and vanadium in incineration bottom ash - Leaching behavior and conclusions for treatment processes. Detritus. 16:75–81. https://doi.org/10.31025/2611-4135/2021.15115
8. Kalbe U, Simon F-G (2020) Potential use of incineration bottom ash in construction: evaluation of the environmental impact. Waste Biomass Valoriz 11(12):7055–7065. https://doi.org/10.1007/s12649-020-01086-2
9. Zhang Y, Ding C, Gong D, Deng Y, Huang Y, Zheng J, Xiong S, Tang R, Wang Y, Su L (2021) A review of the environmental chemical behavior, detection and treatment of antimony. Environ Technol Innov 24:102026. https://doi.org/10.1016/j.eti.2021.102026
10. Diquattro S, Castaldi P, Ritch S, Juhasz AL, Brunetti G, Scheckel KG, Garau G, Lombi E (2021) Insights into the fate of antimony (Sb) in contaminated soils: ageing influence on Sb mobility, bioavailability, bioaccessibility and speciation. Sci Total Environ. https://doi.org/10.1016/j.scitotenv.2021.145354
11. Bolan N, Kumar M, Singh E, Kumar A, Singh L, Kumar S, Keerthanan S, Hoang SA, El-Naggar A, Vithanage M, Sarkar B, Wijesekara H, Diyabalanage S, Sooriyakumar P, Vinu A, Wang H, Kirkham MB, Shaheen SM, Rinklebe J, Siddique KHM (2022) Antimony contamination and its risk management in complex environmental settings: a review. Environ Int 158:106908. https://doi.org/10.1016/j.envint.2021.106908
12. Rinklebe J (ed) (2023) Vanadium in soils and plants. CRC Press, Boca Raton
13. Gustafsson JP (2019) Vanadium geochemistry in the biogeosphere –speciation, solid-solution interactions, and ecotoxicity. Appl Geochem 102:1–25. https://doi.org/10.1016/j.apgeochem.2018.12.027
14. Watt JAJ, Burke IT, Edwards RA, Malcolm HM, Mayes WM, Olszewska JP, Pan G, Graham MC, Heal KV, Rose NL, Turner SD, Spears BM (2018) Vanadium: A Re-Emerging environmental hazard. Environ Sci Technol 52(21):11973–11974. https://doi.org/10.1021/acs.est.8b05560
15. Kjølholt J, Stuer-Lauridsen F, Mogensen AS, Havelund S (2003) The elements in the second rank—an environmental problem now or in the future. Danish Environmental Protection Agency
16. Takaoka M, Yamamoto T, Tanaka T, Takeda N, Oshita K, Uruga T (2005) Direct speciation of lead, zinc and antimony in fly ash from waste treatment facilities by XAFS spectroscopy. Phys Scr. https://doi.org/10.1238/physica.topical.115a00943
17. Okkenhaug G, Zhu Y-G, Luo L, Lei M, Li X, Mulder J (2011) Distribution, speciation and availability of antimony (Sb) in soils and terrestrial plants from an active Sb mining area. Environ Pollut 159(10):2427–2434. https://doi.org/10.1016/j.envpol.2011.06.028
18. Verbeeck M, Moens C, Gustafsson JP (2021) Mechanisms of antimony ageing in soils: An XAS study. Appl Geochem. https://doi.org/10.1016/j.apgeochem.2021.104936
19. Bennett WW, Lombi E, Burton ED, Johnston SG, Kappen P, Howard DL, Canfield DE (2018) Synchrotron X-ray spectroscopy for investigating vanadium speciation in marine sediment: limitations and opportunities. J Anal At Spectrom 33(10):1689–1699. https://doi.org/10.1039/C8JA00231B
20. Burke IT, Mayes WM, Peacock CL, Brown AP, Jarvis AP, Gruiz K (2012) Speciation of arsenic, chromium, and vanadium in red mud samples from the ajka spill site, Hungary. Environ Sci Technol 46(6):3085–3092. https://doi.org/10.1021/es3003475
21. Proux O, Lahera E, Del Net W, Kieffer I, Rovezzi M, Testemale D, Irar M, Thomas S, Aguilar-Tapia A, Bazarkina EF, Prat A, Tella M, Auffan M, Rose J, Hazemann J-L (2017) High-energy resolution fluorescence detected X-Ray absorption spectroscopy: a powerful new structural tool in environmental biogeochemistry sciences. J Environ Qual 46(6):1146–1157. https://doi.org/10.2134/jeq2017.01.0023
22. Rockenberger J, zum Felde U, Tischer M, Tröger L, Haase M, Weller H (2000) Near edge X-ray absorption fine structure measurements (XANES) and extended x-ray absorption fine structure measurements (EXAFS) of the valence state and coordination of antimony in doped nanocrystalline SnO2. J Chem Phys 112(9):4296–4304. https://doi.org/10.1063/1.480975
23. Lahlil S, Biron I, Cotte M, Susini J (2010) New insight on the in situ crystallization of calcium antimonate opacified glass during the Roman period. Appl Phys A 100(3):683–692. https://doi.org/10.1007/s00339-010-5650-z
24. Martin RR, Shotyk WS, Naftel SJ, Ablett JM, Northrup P (2010) Speciation of antimony in polyethylene terephthalate bottles. X-Ray Spectrom 39(4):257–259. https://doi.org/10.1002/xrs.1241
25. Kilias SP, Gousgouni M, Godelitsas A, Gamaletsos P, Mertzimekis TJ, Nomikou P, Argyraki A, Goettlicher J, Steininger R, Papanikolaou D (2016) Antimony fixation in solid phases at the hydrothermal field of Kolumbo submarine arc-volcano (Santorini): deposition model and environmental implications. Bull Geol Soc Greece 50(4):2200–2209. https://doi.org/10.12681/bgsg.14276
26. Borca CN, Huthwelker T, Filella M (2024) A step towards understanding plastic complexity: antimony speciation in consumer plastics and synthetic textiles revealed by XAS. J Environ Sci. https://doi.org/10.1016/j.jes.2024.02.006
27. Caliebe WA, Murzin V, Kalinko A, Görlitz M (2019) High-flux XAFS-beamline P64 at PETRA III. AIP Conf Proc 2054(1):060031. https://doi.org/10.1063/1.5084662
28. Rovezzi M, Harris A, Detlefs B, Bohdan T, Svyazhin A, Santambrogio A, Degler D, Baran R, Reynier B, Noguera Crespo P, Heyman C, Van Der Kleij H-P, Van Vaerenbergh P, Marion P, Vitoux H, Lapras C, Verbeni R, Kocsis MM, Manceau A, Glatzel P (2020) TEXS: in-vacuum tender X-ray emission spectrometer with 11 Johansson crystal analyzers. J Synchrotron Radiat 27(3):813–826. https://doi.org/10.1107/S160057752000243X
29. Vogel C, Simon F-G, Scholz P (2023) EV-511: The chemical state of antimony and vanadium species in municipal solid waste incineration bottom ash. European synchroton Radiation Facility ESRF, Grenoble
30. Calvin S (2013) Furst KE XAFS for everyone. CRC Press Inc., Boca Raton

31. Gmelin (1967) Vanadium, Teil B, in *Gmelins Handbuch der Anorganischen Chemie*
32. Sun X, Li J, Zhao X, Zhu B, Zhang G (2016) A review on the management of municipal solid waste fly ash in AMERICAN. Proc Environ Sci 31:535–540. https://doi.org/10.1016/j.proenv.2016.02.079
33. Okkenhaug G, Almås ÅR, Morin N, Hale SE, Arp HPH (2015) The presence and leachability of antimony in different wastes and waste handling facilities in Norway. Environ Sci Process Impacts 17(11):1880–1891. https://doi.org/10.1039/C5EM00210A
34. Filella M (2020) Antimony and PET bottles: checking facts. Chemosphere 261:127732. https://doi.org/10.1016/j.chemosphere.2020.127732
35. Levchik SV (2007) Introduction to flame retardancy and polymer flammability. In: Morgan AB, Wilkie CA (eds) Flame retardant polymer nanocomposites. Wiley, New York, pp 1–29. https://doi.org/10.1002/9780470109038.ch1
36. Cornelis G, Van Gerven T, Vandecasteele C (2006) Antimony leaching from uncarbonated and carbonated MSWI bottom ash. J Hazard Mater 137(3):1284–1292. https://doi.org/10.1016/j.jhazmat.2006.04.048
37. Bordage A, Balan E, de Villiers JPR, Cromarty R, Juhin A, Carvallo C, Calas G, Sunder Raju PV, Glatzel P (2011) V oxidation state in Fe–Ti oxides by high-energy resolution fluorescence-detected X-ray absorption spectroscopy. Phys Chem Miner 38(6):449–458. https://doi.org/10.1007/s00269-011-0418-3
38. Baker TN (2009) Processes, microstructure and properties of vanadium microalloyed steels. Mater Sci Technol 25(9):1083–1107. https://doi.org/10.1179/174328409X453253
39. Bauer G, Güther V, Hess H, Otto A, Roidl O, Roller H, Sattelberger S (1996) Vanadium and vanadium compounds. In: Ullmann‘s encyclopedia of industrial chemistry. VCH Verlagsgesellschaft, Weinheim
40. Blasenbauer D, Huber F, Lederer J, Quina MJ, Blanc-Biscarat D, Bogush A, Bontempi E, Blondeau J, Chimenos JM, Dahlbo H, Fagerqvist J, Giro-Paloma J, Hjelmar O, Hyks J, Keaney J, Lupsea-Toader M, O'Caollai CJ, Orupõld K, Pająk T, Simon F-G, Svecova L, Šyc M, Ulvang R, Vaajasaari K, van Caneghem J, van Zomeren A, Vasarevičius S, Wégner K, Fellner J (2020) Legal situation and current practice of waste incineration bottom ash utilisation in Europe. Waste Manag 102:868–883. https://doi.org/10.1016/j.wasman.2019.11.031
41. Bundesregierung, (2021) Verordnung zur Einführung einer Ersatzbaustoffverordnung, zur Neufassung der Bundes-Bodenschutz- und Altlastenverordnung und zur Änderung der Deponieverordnung und der Gewerbeabfallverordnung. Bundesgesetzblatt Teil I(43):2598–2752